WIN 55,212-2 shows anti-inflammatory and survival properties in human iPSC-derived cardiomyocytes infected with SARS-CoV-2

Luiz Guilherme H. S. Aragão[1¶], Júlia T. Oliveira[1¶], Jairo R. Temerozo[2,3], Mayara A. Mendes[1], José Alexandre Salerno[1,10], Carolina da S. G. Pedrosa[1], Teresa Puig-Pijuan[1,8], Carla P. Veríssimo[10], Isis M. Ornelas[1], Thayana Torquato[1], Gabriela Vitória[1], Carolina Q. Sacramento[4,5], Natalia Fintelman-Rodrigues[4,5], Suelen da Silva Gomes Dias[4], Vinicius Cardoso Soares[4,6], Leticia R. Q. Souza[1], Karina Karmirian[1,10], Livia Goto-Silva[1], Diogo Biagi[7], Estela M. Cruvinel[7], Rafael Dariolli[7,9], Daniel R. Furtado[1], Patrícia T. Bozza[4], Helena L. Borges[10], Thiago Moreno L. Souza[4,5], Marília Zaluar P. Guimarães[1,10,&*] & Stevens Rehen[1,11,&*]

[1] D'Or Institute for Research and Education (IDOR), Rio de Janeiro, RJ, Brazil.

[2] National Institute for Science and Technology on Neuroimmunomodulation (INCT/NIM), Oswaldo Cruz Institute (IOC), Oswaldo Cruz Foundation (Fiocruz), Rio de Janeiro, RJ, Brazil.

[3] Laboratory on Thymus Research, Oswaldo Cruz Institute (IOC), Oswaldo Cruz Foundation (Fiocruz), Rio de Janeiro, RJ, Brazil.

[4] Laboratory of Immunopharmacology, Oswaldo Cruz Institute (IOC), Oswaldo Cruz Foundation (Fiocruz), Rio de Janeiro, RJ, Brazil.

[5] National Institute for Science and Technology on Innovation in Diseases of Neglected Populations (INCT/IDPN), Center for Technological Development in Health (CDTS), Oswaldo Cruz Foundation (Fiocruz), Rio de Janeiro, RJ, Brazil.

[6] Program of Immunology and Inflammation, Federal University of Rio de Janeiro, UFRJ, Rio de Janeiro, RJ, Brazil.

[7] Pluricell Biotech, São Paulo, SP, Brazil.

[8] Carlos Chagas Filho Institute of Biophysics, Federal University of Rio de Janeiro (UFRJ), Rio de Janeiro, RJ, Brazil.

[9] Department of Pharmacological Sciences, Icahn School of Medicine at Mount Sinai, New York, NY, United States.

[10] Institute of Biomedical Sciences, Federal University of Rio de Janeiro (UFRJ), Rio de Janeiro, RJ, Brazil.

[11] Department of Genetics, Institute of Biology, Federal University of Rio de Janeiro (UFRJ), Rio de Janeiro, RJ, Brazil.

¶ These authors contributed equally to this work

& These authors contributed equally to this work.

*Corresponding author: srehen@lance-ufrj.org, UFRJ and D'Or Institute for Research and Education

Abstract

Coronavirus disease 2019 (COVID-19) is caused by severe acute respiratory syndrome coronavirus 2 (SARS-CoV-2), which can infect several organs, especially impacting respiratory capacity. Among the extrapulmonary manifestations of COVID-19 is myocardial injury, which is associated with a high risk of mortality. Myocardial injury, caused directly or indirectly by SARS-CoV-2 infection, can be triggered by inflammatory processes that cause damage to the heart tissue. Since one of the hallmarks of severe COVID-19 is the “cytokine storm”, strategies to control inflammation caused by SARS-CoV-2 infection have been considered. Cannabinoids are known to have anti-inflammatory properties by negatively modulating the release of pro-inflammatory cytokines. Herein, we investigated the effects of the cannabinoid agonist WIN 55,212-2 (WIN) in human iPSC-derived cardiomyocytes (hiPSC-CMs) infected with SARS-CoV-2. WIN did not modify angiotensin-converting enzyme II protein levels, nor reduced viral infection and replication in hiPSC-CMs. On the other hand, WIN reduced the levels of interleukins 6, 8, 18 and tumor necrosis factor-alpha (TNF-α) released by infected cells, and attenuated cytotoxic damage measured by the release of lactate dehydrogenase (LDH). Our findings suggest that cannabinoids should be further explored as a complementary therapeutic tool for reducing inflammation in COVID-19 patients.

Introduction

The causative agent of Coronavirus disease 2019 (COVID-19), SARS-CoV-2, can affect multiple organs, including lungs, nervous system (Carod-Artal, 2020), digestive system (Chen et al., 2020b), urinary system (Puelles et al., 2020), skin (Mahé et al., 2020; Diaz-Guimaraens et al., 2020) and heart (Maisch, 2020; Varga et al., 2020; Zheng et al., 2020).

A *post-mortem* study of a child with COVID-19 revealed diffuse myocardial interstitial inflammation with immune cells infiltration and necrosis (Dolhnikoff, 2020). Recently, we showed cardiac damage, namely microthrombi in small arteries and focal mild lymphocytic infiltrate in the ventricles, of an infant who died of COVID-19 (Gomes et al., 2020). Another study detected SARS-CoV-2 in myocardial tissue, which expressed inflammatory mediators, such as tumor necrosis factor-alpha (TNF-α), interferon-gamma (IFN-γ), chemokine ligand 5, as well as interleukin (IL) -6, -8, and -18 (Lindner et al., 2020). Additionally, patients with COVID-19 presented elevated levels of creatine kinase and lactate dehydrogenase (LDH) activity, which are biomarkers of heart injury (Chen et al., 2020b; Zhou et al., 2020).

High expression of Angiotensin-Converting Enzyme II (ACE2) in the heart has been correlated with severe COVID-19 and susceptibility of patients with pre-existing cardiac conditions (Chen et al., 2020a; Thum, 2020; Sharma et al., 2020; Dariolli et al., 2021). *In vitro* studies have shown that SARS-CoV-2 infects iPSC-derived cardiomyocytes (hiPSC-CMs) through ACE2 (Sharma et al., 2020; Dariolli et al., 2021), leading to upregulation of inflammation-related genes, including IL-6, IL-8, and TNF-α (Wong et al., 2020; Kwon et al., 2020). The increase in proinflammatory cytokines can cause several adverse effects in cardiomyocytes including arrhythmia

(Keck et al., 2019), cellular hypertrophy (Smeets et al., 2008), cell death (Wang et al., 2016), conversion of fibroblasts into myofibroblasts (Wang et al., 2016) and alteration of action potentials' duration (Aromolaran et al., 2018). The correlation between inflammation and heart damage in *post-mortem* and in *in vitro* studies points to the need for finding strategies that mitigate direct SARS-CoV-2 cardiac outcomes.

For many centuries *Cannabis sp*. has been used for medicinal purposes and, more recently, it has been investigated as a therapeutic agent for cardiovascular diseases (Mendizábal & Adler-Graschinsky, 2007; Pacher et al., 2018). *Cannabis* has several known compounds, named phytocannabinoids, including delta-9-tetrahydrocannabinol (THC), which is the most abundant and the main psychoactive ingredient, followed in amount by cannabidiol (CBD). Besides phytocannabinoids, there is intensive research on endocannabinoids, such as anandamide and 2-arachidonoylglycerol, and synthetic cannabinoids, such as WIN 55,212–2 (WIN). Nguyen et al., (2021) showed the potential of cannabinoids to decrease SARS-CoV-2 infection, viral replication, and inflammation that are directly related to COVID-19 severity. Treatment with *Cannabis* extracts decreased ACE2 expression in oral, intestinal, and airway epithelia *in vitro* (Wang et al., 2020). It is noteworthy that cannabinoids have anti-inflammatory properties and exert their biological effect mainly by interaction with the cannabinoid receptors type 1 (CB1) and/or type 2 (CB2), to both of which WIN has high affinity and efficacy (Devane et al., 1988; Munro, Thomas & Abu-Shaar, 1993; Felder et al., 1995; Soethoudt et al. 2017; Sachdev et al., 2019). For instance, WIN was shown to reduce the number of lipopolysaccharide-activated microglia in the brain of an animal model of chronic inflammation (Marchalant, Rosi & Wenk, 2007). Another work showed that WIN decreased TNF-α and IL-6 plasma levels and myeloperoxidase activity in mice with experimental colitis (Feng et al., 2016). An

extract fraction from *Cannabis sativa* Arbel strain enriched in CBD, cannabigerol and tetrahydrocannabivarin presented anti-inflammatory activity in lung epithelial cells treated with TNF-α but another fraction with high CBD containing terpenes in addition to phytocannabinoids enhanced proinflammatory parameters of macrophages (Anil et al., 2021). Additionally, high-CBD *Cannabis sativa* extracts presented anti-inflammatory properties in the epithelia pretreated with TNF-α and IFN-γ (Lei et al., 2020). Smith et al. (2000) showed that treatment with WIN decreased serum TNF-α and IL-12 and increased IL-10 through the CB1 receptor in mice treated with lipopolysaccharide (Smith, Terminelli & Denhardt, 2000). Investigating the anti-inflammatory potential of *Cannabis sativa* in cardiomyocytes is important because the "cytokine storm" is a hallmark of COVID-19 and the cardiovascular system is mostly affected in severe cases (Unudurthi et al., 2020). To date, the effects of cannabinoids in human cardiomyocytes infected with SARS-CoV-2 has not been addressed.

In this work, we aimed to investigate the effects of a synthetic cannabinoid, that acts as a mixed CB1/CB2 receptors agonist, in hiPSC-CMs infected by SARS-CoV-2. WIN presented anti-inflammatory and protective properties by reducing the levels of proinflammatory cytokines and cell death in hiPSC-CM but did neither modulate ACE2 nor reduced SARS-CoV-2 infection and replication. Our data suggest that the anti-inflammatory and protective properties of WIN may be used to control inflammation and tissue damage during SARS-CoV-2 infection of heart cells.

Materials & Methods

Chemical

WIN 55,212-2 mesylate was purchased from TargetMol (T4458). Stock solutions were prepared using 100% dimethyl sulfoxide (DMSO; D2650 - Sigma-Aldrich) and sterile-filtered. The final concentration of DMSO in work solution was 0.01%.

iPS-Cardiomyocyte differentiation and purification

hiPSC-CMs were purchased from Pluricell (São Paulo, Brazil) and used between day 25 and day 35 of differentiation. The hiPSC-CMs used here were generated and previously characterized *in vitro* by Cruvinel et al. (2020). Briefly, the enrichment of the cardiomyocyte population was assessed by flow cytometry and immunofluorescence of TNNT2, a specific marker, which revealed that, on average, 88.4% (+/- 8.4%) cells were positive cells (Fig S3). hiPSC-CMs were handled in four different groups: MOCK and SARS-CoV-2 (SARS-CoV-2 infection without WIN), which were also analyzed as controls in Salerno et al. (2021), MOCK WIN (no SARS-CoV-2 infection + WIN), and SARS-CoV-2 WIN (SARS-Cov-2 infection + WIN). All WIN-treated hiPSC-CMs were pretreated for 24 hours with 1 µM WIN. Fresh culture medium with (or without) 1 µM WIN, combined or not with SARS-CoV-2, was added for 24 hours to each experimental group, respectively.

SARS-CoV-2 propagation

SARS-CoV-2 was expanded in Vero E6 cells from an isolate of a nasopharyngeal swab obtained from a confirmed case in Rio de Janeiro, Brazil (GenBank accession no. MT710714). Viral isolation was performed after a single passage in 150 cm^2 flasks cultured with high glucose DMEM plus 2% FBS. Observations for cytopathic effects

were performed daily and peaked 4 to 5 days after infection. All procedures related to virus culture were handled in biosafety level 3 (BSL3) multi-user facilities according to WHO guidelines. Virus titers were determined as plaque-forming units (PFU/mL) as explained below, and virus stocks were kept at -80°C.

SARS-CoV-2 titration

For virus titration, monolayers of Vero E6 cells (2 x 10^4 cell/well) in 96-well plates were infected with serial dilutions of supernatants containing SARS-CoV-2 for 1 hour at 37°C. A semi-solid high glucose DMEM medium containing 2% FSB and 2.4% carboxymethylcellulose was added and cultures were incubated for 3 days at 37 °C. Then, the cells were fixed with 10% formalin for 2 hours at room temperature. The cell monolayer was stained with 0.04% solution of crystal violet in 20% ethanol for 1 hour. Plaque numbers were scored in at least 3 replicates per dilution by independent readers blinded to the experimental group and the virus titers were determined by plaque-forming units (PFU) per milliliter.

SARS-CoV-2 infection

hiPSC-CMs were infected with SARS-CoV-2 at a multiplicity of infection (MOI) of 0.1 in high glucose DMEM without serum. After 1 hour, cells were washed and incubated with Complete Medium with or without treatments for 48-72h. Next, the supernatant was collected, and cells were fixed with 4% paraformaldehyde (PFA) solution for posterior analysis.

Measurement of cytokines mediators and LDH cytotoxicity

Cytokines (IL-6, IL-7, IL-8, and TNF-α) were quantified in the supernatants from hiPSC-CMs samples by ELISA (R&D Systems) following manufacturer's instructions.

The analysis of data was performed using software provided by the manufacturer (Bio-Rad Laboratories, USA). A range of 0.51–8,000 pg/mL recombinant cytokines was used to establish standard curves and the sensitivity of the assay. Cell death was determined according to the activity of lactate dehydrogenase (LDH) in the culture supernatants using a CytoTox® Kit (Promega, USA) according to the manufacturer's instructions.

Gene expression analysis

Qualitative endpoint PCR reactions were executed with the following primer sequences: CB1 (forward 5'-ATGTGGACCATAGCCATTGTG-3'; reverse: 5'-CCGATCCAGAACATCAGGTAGG-3') and CB2 (forward 5'-GCTATCCACCTTCCTACAAAGC-3'; reverse: 5'- CTCAGCAGGTAGTCATTGGGG-3'). Glyceraldehyde-3-phosphate Dehydrogenase (GAPDH; forward: 5'-TTCGACAGTCAGCCGCATC-3'; reverse: 5'-GACTCCACGACGTACTCAGC-3') was used as the endogenous housekeeping control gene. Each PCR reaction was performed in a 10 µL mixture containing 0.25 U GoTaq G2 Hot Start Polymerase (Promega), 1x GoTaq G2 Buffer, 1.5 mM MgCl2 (Invitrogen), 200 nM of each primer (forward and reverse), 200 µM dNTP mixture containing the four deoxyribonucleotides (dATP, dCTP, dTTP, and dGTP), and 10 ng of cDNA template. Appropriate negative controls and genomic DNA positive controls were incorporated into each experiment. Amplification thermal program included an initial denaturation step of 95°C for 3 minutes and 40 cycles of 95°C for 15 seconds, 60°C for 15 seconds and 72°C for 15 seconds using the ProFlexTM PCR System Thermal Cycler (Applied Biosystems). Subsequently, the total amount of PCR product was separated by electrophoresis at

110 V for 40 minutes in 1.8% agarose gel diluted in 1× Tris-acetate EDTA buffer (w/v) and stained with 0.01% of SYBR Safe (Thermo Fisher).

For real-time quantitative PCR, the reactions were carried out in triplicates in a reaction mixture containing 1x GoTaq qPCR MasterMix (Promega Corporation), 300 nM CXR Reference Dye, a final concentration of 200 nM of each (forward and reverse) SYBR green-designed primers (Thermo Fisher Scientific), and 10 ng of cDNA template per reaction. Appropriate negative controls were added in each run. The relative expression of the genes of interest: ACE2 (forward: 5'-CGAAGCCGAAGACCTGTTCTA-3'; reverse: 5'-GGGCAAGTGTGGACTGTTCC-3'), MYH6 (forward: 5'- GCCCTTTGACATTCGCACTG-3'; reverse: 5'-GGTTTCAGCAATGACCTTGCC-3'), MYH7 (forward: 5'-TCACCAACAACCCCTACGATT-3'; reverse: 5'-CTCCTCAGCGTCATCAATGGA-3') was normalized by human reference genes: Glyceraldehyde-3-phosphate Dehydrogenase (GAPDH; forward: 5'-GCCCTCAACGACCACTTTG-3'; reverse: 5'-CCACCACCCTGTTGCTGTAG-3') and Hypoxanthine Phosphoribosyltransferase 1 (HPRT-1; forward 5'-CGTCGTGATTAGTGATGATGAACC-3'; reverse: 5'-AGAGGGCTACAATGTGATGGC-3'). The reactions were performed on a StepOnePlusTM Real-Time PCR System thermocycler (Applied Biosystems). Thermal cycling program comprised of a denaturing step at 95°C for 3 minutes, followed by 40 cycling stages at 95°C for 15 seconds, 57°C for 15 seconds, 72°C for 15 seconds and melt curve stage 95 °C, 15 seconds; 60 °C, 1 minutes; 95 °C, 15 seconds. Data analysis was performed with LinRegPCR quantitative PCR data analysis program v. 2020.0, as previously described.

Immunofluorescence staining

SARS-CoV-2-infected and mock-treated hiPSC-CMs were fixed using 4% paraformaldehyde solution (Sigma-Aldrich, EUA) for 1 hour and stored at 4ºC. Next, cells were washed with PBS and then incubated with permeabilization/blocking solution (0.3% Triton X-100 / 1% bovine serum albumin + 3% normal goat serum) for 1 hour. Cardiomyocytes were incubated with primary antibodies diluted in a blocking buffer solution at 4º overnight: anti-SARS-CoV-2 convalescent serum from a positive COVID-19 patient (1:1000) and anti-cardiac troponin T (TNNT2) (1:500, MA5-12960 - Invitrogen). Afterwards, cardiomyocytes were incubated with the secondary antibody diluted in a blocking buffer solution: goat anti-Human Alexa Fluor 647 (1:400; A-21445 - Invitrogen) and goat anti-Mouse 594 (1:400; A-11032 - Invitrogen) for 1 hour. Actin filaments were stained with Alexa Fluor 568 phalloidin (1:10; A-12380 - Life Technologies) for 1 hour. Nuclei were stained with 300 nM 4'-6-diamino-2-phenylindole (DAPI) for 5 minutes and each well was mounted with two drops of 50% PBS-Glycerol. Images (at least 10 fields per well) of hiPSC-CMs were acquired using Operetta® High-Content Imaging System (Perkin Elmer) with a 20x long working distance (WD) objective lens. A Leica TCS-SP8 confocal microscope was used to acquire images of hiPSC-CMs immunostained for TNNT2 and F-actin with the 63x objective (Fig S3).

Neutral red uptake cell viability assay

Briefly, hiPSC-CMs were seeded in 96-well plates. After reaching 80–90% confluency, cells were exposed to concentrations of WIN ranging between 10 nM-10 µM for 72 hours. Next, the medium was replaced, cells were washed with PBS 1x and 200 µL of neutral red dye diluted in the hiPSC-CMs medium was added to each well at a final

concentration of 0.05 mg/mL. After 3 hours of incubation at 37ºC, neutral red dye was removed, and the cells were washed again. Then, 100 µL of the neutral red desorb solution was added (1% acetic acid-49% ethanol) to the wells, followed by 20 minutes in orbital shaking. Absorbance at 540 nm was measured with a Tecan Infinite® 200 PRO (Life Sciences, Switzerland) spectrophotometer.

Western Blotting

Twenty-four hours after treatment with WIN of hiPSC-CMs in 24-well plates, 100 µL of sample buffer without bromophenol blue (62.5 mM Tris-HCl, pH 6.8, containing 10% glycerol, 2% SDS, and 5% 2-mercaptoethanol) was added in each well, and a cell scraper was used to help lyse the cells. Cell extracts were transferred to an Eppendorf tube, boiled at 95ºC for 5 minutes, and centrifuged at 4ºC 16,000 x*g* for 15 minutes to collect the supernatant. Protein content was estimated using the Bio-Rad Protein Assay (# 5000006, Biorad). Next, bromophenol blue (0.02%) was added, and extracted samples (40 µg/lane) were separated by an 8% SDS polyacrylamide gel electrophoresis and transferred to polyvinylidene difluoride (PVDF) membranes. The membranes were blocked in 5% non-fat milk in Tris Buffered Saline with 0.1% Tween-20 (TBS-T) for 1 hour at room temperature. Then, membranes were incubated overnight at 4ºC with primary antibodies anti-ACE2 (1: 1000; MA5-32307 - Thermo Fisher), anti-CB1 (1:300, CSB-PA007048, Cusabio), and anti-ACTIN (1:2000; MAB1501, Millipore), diluted in TBS-T with 5% non-fat milk. Membranes were washed and incubated with peroxidase-conjugated antibodies IgG (H + L), HRP-conjugate: goat anti-mouse (1: 10.000, G21040, Molecular Probes), goat anti-rabbit (1: 10.000, G21234, Molecular Probes), and rabbit anti-goat (1: 2.000, 61-1620, Invitrogen) for 2 hours at room temperature. The signals were developed using an ECL Prime Western Blotting System (# GERPN2232, Sigma) for 5 minutes, and chemiluminescence was

296 detected with an Odyssey-FC Imaging System® (LI-COR Biosciences, EUA). After
297 CB1 or CB2 detection a stripping protocol was used on the membranes for further
298 detection of actin. Membranes were incubated with a stripping buffer (pH 2.2, 200 mM
299 glycine, 0.1% SDS, and 1% Tween-20) for three cycles of 10 minutes. Next, the buffer
300 was discarded, and the membranes were washed three times with PBS and three
301 times for 5 minutes with 0.1% TBS-T. Then, membranes were blocked again and
302 proceeded with the above-described steps.

303 Statistics

304 Statistical analyses were performed using GraphPadPrism software version 8.0
305 (GraphPad, EUA). Results were expressed as the mean and standard error of the
306 mean (SEM). For comparisons between two experimental groups, unpaired two-tailed
307 Student's t-test or Mann-Whitney U test was used, whereas two-way analysis of
308 variance (ANOVA) or Kruskal-Wallis test followed by Tukey's test was used for
309 comparisons between three or more groups. A p-value smaller than 0.05 was
310 accepted as statistically significant.

311 Ethics Statement

312 Approved by the Research Ethics Committee of D'Or Institute of Research and
313 Education (IDOR) 39474020.8.0000.5249.

314

315

316

317

Results

1. Human cardiomyocytes express cannabinoid receptor 1 but WIN does not modulate ACE2 expression

As a first step to investigate the influence of cannabinoid receptors in SARS-CoV-2 infection of human cardiomyocytes, we checked whether hiPSC-CMs expressed CB1 and CB2 receptors. We found that hiPSC-CMs express only CB1 receptor mRNA (Fig S1A), which was confirmed by CB1 protein expression (Fig S1B). The banding pattern observed in the hiPSC-CMs was similar to the mouse hippocampus sample (positive control) and consistent with what was observed in samples from other CNS regions (Medina-Vera et al., 2020).

WIN is an agonist at the CB1 and CB2 receptors with a higher affinity to them than other cannabinoids (Acheson et al., 2011; Sachdev., 2019), including THC (Felder et al. 1995) and therefore it is an useful pharmacological tool to study cannabinoid receptor activation. Beforehand, we tested multiple WIN concentrations in readouts of cellular toxicity and permanent cardiac hypertrophy. We found that WIN did not reduce cell viability in concentrations up to 1 µM (Fig S3A). Also, compared with control, 1 µM WIN did not increase MYH6 and MYH7 mRNA levels (Fig S3B), genes that, when upregulated, may indicate cardiac hypertrophy *in vitro* (Wenzel, 1967; Rahmatollahi et al., 2016; Albakri, 2019). Therefore, we chose 1 µM WIN as the usage concentration for further assays since it caused neither cell death nor changes in gene expression related to hypertrophy.

After confirming that hiPSC-CMs express CB1 and ACE2 (Salerno et al., 2021), we asked whether WIN modulates ACE2 expression and, subsequently, influences SARS-CoV-2 infection within hiPSC-CMs. hiPSC-CMs were pretreated with 1 µM WIN

for 24 hours and analyzed for both mRNA and protein levels of ACE2. We observed that WIN-treated (1.15 ± 0.07 A.U.) and untreated (0.98 ± 0.11 A.U.) hiPSC-CMs had comparable levels of ACE2 mRNA whereas ACE2 protein levels in WIN treated cells whereas ACE2 protein levels in WIN treated cells was 1.16 ± 0.39, normalized to control (Fig 1A, B and C, and Fig S2).

2. WIN does not influence SARS-CoV-2 infection and replication in hiPSC-CMs

Next, we asked whether WIN could reduce hiPSC-CMs SARS-CoV-2 infection by mechanisms other than ACE2 modulation. For this, cells were pretreated with 1 µM WIN for 24 hours and infected with SARS-CoV-2 at a multiplicity of infection (MOI) of 0.1 for 1 hour, and the PFU analyzed 48 hours later. In this study, we defined the use of MOI 0.1 for all experiments because this MOI had already been successfully used to infect hiPSC-CMs with SARS-CoV-2 (Sharma et al., 2020). Additionally, MOIs above 0.1 may not be a clinically plausible viral load found *in vivo*. Forty-eight hours after infection, we quantified convalescent serum (CS)-immunostaining and, as expected, we found that cells in the MOCK group had no CS immunoreactivity. Among the SARS-CoV-2-infected cells, those pretreated with WIN had a comparable percentage of infected cells (WIN SARS-CoV-2; 30±15%) to those untreated (SARS-CoV-2; 26±12%) (Fig 2A and B).

Since viral infection and replication are correlated but orchestrated by different mechanisms, we asked whether WIN could decrease SARS-CoV-2 replication in hiPSC-CMs. We observed that despite a decrease in average viral titer when comparing SARS-CoV-2 WIN ($6.99 \times 10^5 \pm 4.39 \times 10^5$ PFU/mL) with SARS-CoV-2 ($2.18 \times 10^6 \pm 9.96 \times 10^5$ PFU/mL), the difference was not statistically significant (Fig 2C).

366 **3. WIN reduces the secretion of inflammatory cytokines in SARS-CoV-2-infected**
367 **hiPSC-CMs**

368 The “cytokine storm” is a hallmark of severe COVID-19 cases and cannabinoids have
369 well-known anti-inflammatory properties. We asked whether WIN could reduce the
370 release of the inflammatory cytokines IL-6, IL-8, TNF-α by hiPSC-CMs *in vitro*. Cells
371 were pretreated with 1 µM WIN for 24 hours, infected for 1 hour, and incubated further
372 for 24, 48, and 72 hours. Then, the media were harvested at each time point for
373 analysis. We found that cells infected with SARS-CoV-2 released higher levels of
374 cytokines when compared with MOCK, with the exception of IL-8 at 24 and IL-6 at 72
375 hours post-infection (Fig 3A, B, and C). Most importantly, in all conditions that
376 significantly augmented the release of these pro-inflammatory cytokines, WIN was
377 able to prevent this increase (Fig 3A, B, and C). Of note, whereas the basal amount
378 of cytokines tended to increase during culture time as they accumulated without media
379 changes, WIN did not significantly affect this basal release by comparing MOCK and
380 MOCK WIN groups.

381 **4. WIN reduces cell death in SARS-CoV-2- infected hiPSC-CMs**

382 It has been previously reported that SARS-CoV-2 infection causes apoptosis in
383 hiPSC-CMs (Perez-Bermejo et al., 2021, p.). As cannabinoids can be protective in
384 some tissues, we investigated whether WIN would protect hiPSC-CMs from cell death.
385 Cells were pretreated with 1 µM WIN for 24 hours, infected for 1 hour, and cultivated
386 for additional 24, 48, and 72 hours and LDH was measured in the media at these
387 different time points. Forty-eight and 72 hours after the infection with SARS-CoV-2
388 without WIN, the release of LDH increased 463% and 174%, respectively, in hiPSC-

CMs. On the other hand, hiPSC-CMs infected with SARS-CoV-2 and exposed to WIN had significantly lower increments of 72% and 40%, respectively (Figure 3D).

Discussion

Cannabinoids have been proposed as potential treatment and prevention of COVID-19, due to their antiviral, cytoprotective and anti-inflammatory properties (Marchalant, Rosi & Wenk, 2007; Rossi et al., 2020; Anil et al., 2021). In this study, we showed that the synthetic CB1/CB2 agonist WIN reduced cell damage in SARS-CoV-2-infected hiPSC-CMs. Additionally, even though cardiomyocytes are not known for evoking robust inflammatory responses, WIN reduced the release of cytokines by these cells following SARS-CoV-2 infection. To our knowledge, this is the first study showing anti-inflammatory and protective properties of a cannabinoid agonist in hiPSC-CMs infected with SARS-CoV-2.

We hypothesized that WIN reduces the levels of ACE2 in hiPSC-CMs, consequently abrogating SARS-CoV-2 infection and viral load in these cells. However, despite hiPSC-CMs expressing ACE2, it only presented a tendency towards an increase which was not modulated by WIN in the conditions studied here. ACE2 is downregulated in SARS-CoV-2 infected tissues (Yan et al., 2020; Gheblawi et al., 2020), which is harmful to the heart since ACE2 has a protective role in the cardiovascular system (Huentelman et al., 2005; Zhong et al., 2010). Studies have shown that agonists of cannabinoid receptors, including WIN, cause vasodilation through the activation of CB1 receptors, and are capable of modulating vasoactive ligands (Sainz-Cort & Heeroma, 2020; Miklós et al., 2021). One possibility for the tendency towards an increase in the levels of ACE2 in WIN-treated hiPSC-CMs is that this cannabinoid agonist could exert a protective role by preventing receptor

413 downregulation. Although it has been previously shown (Wang et al., 2020) that CBD-
414 rich extracts reduced ACE2 mRNA and protein levels in some epithelia *in vitro*
415 following TNF-α insult, this modulation had not been investigated in SARS-CoV-2
416 infected cardiomyocytes until now.

417 Despite evidence of cannabinoid receptors expression in murine embryonic stem cells
418 (Jiang et al., 2007) and human cardiomyocytes (Mukhopadhyay et al., 2010), to our
419 knowledge, this is the first description of the expression of CB1 receptor in hiPSC-
420 CMs. The modulation of cannabinoid receptors in cardiomyocytes has also not been
421 explored yet. Our results showed that WIN did not reduce the infection rate or the viral
422 titer in hiPSC-CMs in the conditions studied here. Several studies have examined the
423 effect of cannabinoids on viral infections, especially regarding the role of CB1 and CB2
424 receptor activation (Reiss, 2010). The CB2 receptor agonist JWH-133 reduced
425 CXCR4-tropic HIV-1 infection of primary CD4+ T cells, whereas the CB1 receptor
426 agonist arachidonoyl-29-chloroethylamide had no effect. In another study with HIV-1-
427 infected primary human monocytes, agonists of CB2 receptors limited viral replication
428 (Ramirez et al., 2013). There is still no consensus on the antiviral mechanisms of
429 cannabinoids, however, it is well-known that the selective activation of the CB2
430 receptor plays a crucial role in the course of viral infection (Rossi et al., 2020). The
431 fact that hiPSC-CMs do not express the CB2 receptor may explain WIN's
432 ineffectiveness in reducing SARS-CoV-2 infection and replication in these cells.
433 Additionally, to date, cannabinoid treatment along with SARS-CoV-2 infection had not
434 been investigated in this cellular model. It is likely that viral infection mechanisms
435 through CB1 and CB2 receptors might vary depending on virus and cell type (Reiss,
436 2010; Tahamtan et al., 2016).

Although immune cells and cardiac fibroblasts are typically the major players in cytokine production under stressed cardiac conditions (Zhong et al., 2010), cardiomyocytes are also a local source of proinflammatory cytokines (Yamauchi-Takihara et al., 1995; Ancey et al., 2002; Kleinbongard, Schulz & Heusch, 2011; Atefi et al., 2011; Bozzi et al., 2019). In this work, hiPSC-CMs released IL-6, IL-8, and TNF-α at baseline levels and SARS-CoV-2 infection increased all cytokines levels. It has been shown that infection of hiPSC-CMs by *Trypanosoma cruzi*, the Chagas' disease pathogen, prompted these cells to produce proinflammatory cytokines that caused autocrine cardiomyocyte dysfunction (Bozzi et al., 2019). Cardiac damage in COVID-19 patients can be attributable to hypoxemia due to respiratory dysfunction (Guo et al., 2020) but also to the “cytokine storm”, which is the uncontrolled systemic inflammatory response likely caused by an imbalance between regulatory and cytotoxic T cells (Meckiff et al., 2020). Even though the “cytokine storm” is one of the hallmarks of SARS-CoV-2 infection (Coperchini et al., 2020), one cannot rule out that cytokines locally released contribute to tissue damage, as seen, for example, in *Trypanosoma cruzi* cardiac infection (Bozzi et al., 2019). Here we found that WIN decreased the levels of IL-6, IL-8, and TNF-α released by SARS-CoV-2-infected hiPSC-CMs. An *in vitro* study of cortical astrocytes treated with Amyloid-$\beta_{1–42}$, which is a neurotoxic protein, showed that WIN reduced TNF-α and IL-1β levels, while preventing cell death (Aguirre-Rueda et al., 2015). In another study, WIN decreased the activity of peroxisome proliferator-activated receptor alpha and TNF-α levels in the heart tissue of mice with cardiac dysfunction (Rahmatollahi et al., 2016), reinforcing its anti-inflammatory and protective properties in cardiac tissue.

THC and WIN are structurally different and accordingly have different efficacies towards activation of cannabinoid signaling pathways (Soethoudt et al., 2017).

462 However, they are both mutual CB1 and CB2 receptor agonists (Compton et al., 1992)
463 and can produce similar pharmacological effects, depending on the assay (Fan et al.,
464 1994). THC presented a protective role against hypoxia in neonatal murine
465 cardiomyocytes by reducing the levels of LDH (Shmist et al., 2006). Since neonatal
466 murine cardiomyocytes expressed CB2, but not CB1, the authors suggest that
467 cardioprotection provided by THC occurs via the CB2 receptor. Herein, we were able
468 to show that hiPSC-CMs expressed only CB1 but not CB2. In human cardiomyocytes,
469 WIN decreased the release of LDH release and this effect could be mediated by CB1,
470 to which WIN has high affinity. Other receptor candidates, such as transient receptor
471 potential vanilloid (TRPV) channels (Freichel et al., 2017) can not be discarded.
472 Nonetheless, the modulation of TRPV channels by WIN occurs at 10 µM or higher
473 (Jeske et al., 2006; Koch et al., 2011), which are, at least, 10 times above the
474 concentration used in our study.

475 **Conclusion**

476 This study showed that pretreatment with a cannabinoid receptor agonist reduced
477 cytotoxicity and proinflammatory cytokines released by human cardiomyocytes
478 infected with SARS-CoV-2. These results suggest that the therapeutic potential of
479 cannabinoids in protecting the heart against SARS-CoV-2 infection should be further
480 explored, in particular regarding selective action on the CB1 receptor.

481 **References**

482 Aguirre-Rueda D, Guerra-Ojeda S, Aldasoro M, Iradi A, Obrador E, Mauricio MD, Vila JM,
483 Marchio P, Valles SL. 2015. WIN 55,212-2, Agonist of Cannabinoid Receptors, Prevents
484 Amyloid β1-42 Effects on Astrocytes in Primary Culture. *PLOS ONE* 10:e0122843. DOI:
485 10.1371/journal.pone.0122843.

Albakri A. 2019. Drugs-related cardiomyopathy: A systematic review and pooled analysis of pathophysiology, diagnosis and clinical management. *Internal Medicine and Care* 3. DOI: 10.15761/IMC.1000129.

Ancey C, Corbi P, Froger J, Delwail A, Wijdenes J, Gascan H, Potreau D, Lecron J-C. 2002. Secretion of IL-6, IL-11 and LIF by human cardiomyocytes in primary culture. *Cytokine* 18:199–205. DOI: 10.1006/cyto.2002.1033.

Anil SM, Shalev N, Vinayaka AC, Nadarajan S, Namdar D, Belausov E, Shoval I, Mani KA, Mechrez G, Koltai H. 2021. Cannabis compounds exhibit anti-inflammatory activity in vitro in COVID-19-related inflammation in lung epithelial cells and pro-inflammatory activity in macrophages. *Scientific Reports* 11:1462. DOI: 10.1038/s41598-021-81049-2.

Aromolaran AS, Srivastava U, Alí A, Chahine M, Lazaro D, El-Sherif N, Capecchi PL, Laghi-Pasini F, Lazzerini PE, Boutjdir M. 2018. Interleukin-6 inhibition of hERG underlies risk for acquired long QT in cardiac and systemic inflammation. *PloS One* 13:e0208321. DOI: 10.1371/journal.pone.0208321.

Atefi G, Zetoune FS, Herron TJ, Jalife J, Bosmann M, Al-Aref R, Sarma JV, Ward PA. 2011. Complement dependency of cardiomyocyte release of mediators during sepsis. *The FASEB Journal* 25:2500–2508. DOI: 10.1096/fj.11-183236.

Bozzi A, Sayed N, Matsa E, Sass G, Neofytou E, Clemons KV, Correa-Oliveira R, Stevens DA, Wu JC. 2019. Using Human Induced Pluripotent Stem Cell-Derived Cardiomyocytes as a Model to Study Trypanosoma cruzi Infection. *Stem Cell Reports* 12:1232–1241. DOI: 10.1016/j.stemcr.2019.04.017.

Carod-Artal FJ. 2020. Neurological complications of coronavirus and COVID-19. *Revista De Neurologia* 70:311–322. DOI: 10.33588/rn.7009.2020179.

Chen L, Li X, Chen M, Feng Y, Xiong C. 2020a. The ACE2 expression in human heart indicates new potential mechanism of heart injury among patients infected with SARS-CoV-2. *Cardiovascular Research* 116:1097–1100. DOI: 10.1093/cvr/cvaa078.

Chen N, Zhou M, Dong X, Qu J, Gong F, Han Y, Qiu Y, Wang J, Liu Y, Wei Y, Xia J, Yu T, Zhang X, Zhang L. 2020b. Epidemiological and clinical characteristics of 99 cases of 2019

514 novel coronavirus pneumonia in Wuhan, China: a descriptive study. *The Lancet* 395:507–
515 513. DOI: 10.1016/S0140-6736(20)30211-7.
516 Compton DR, Gold LH, Ward SJ, Balster RL, Martin BR. 1992. Aminoalkylindole analogs:
517 cannabimimetic activity of a class of compounds structurally distinct from delta 9-
518 tetrahydrocannabinol. *The Journal of Pharmacology and Experimental Therapeutics*
519 263:1118–1126.
520 Dariolli R, Campana C, Gutierrez A, Sobie EA. 2021. In vitro and in silico models to study
521 SARS-CoV-2 infection: integrating experimental and computational tools to mimic
522 "COVID-19 cardiomyocyte" *Frontiers in Physiology* 12. DOI:
523 10.3389/fphys.2021.624185.
524 Devane WA, Dysarz FA, Johnson MR, Melvin LS, Howlett AC. 1988. Determination and
525 characterization of a cannabinoid receptor in rat brain. *Molecular Pharmacology* 34:605–
526 613.
527 Diaz-Guimaraens B, Dominguez-Santas M, Suarez-Valle A, Pindado-Ortega C, Selda-
528 Enriquez G, Bea-Ardebol S, Fernandez-Nieto D. 2020. Petechial Skin Rash Associated
529 With Severe Acute Respiratory Syndrome Coronavirus 2 Infection. *JAMA Dermatology*
530 156:820. DOI: 10.1001/jamadermatol.2020.1741.
531 Dolhnikoff M. 2020. SARS-CoV-2 in cardiac tissue of a child with COVID-19-related
532 multisystem inflammatory syndrome. 4:5.
533 Fan F, Compton DR, Ward S, Melvin L, Martin BR. 1994. Development of cross-tolerance
534 between delta 9-tetrahydrocannabinol, CP 55,940 and WIN 55,212. *The Journal of*
535 *Pharmacology and Experimental Therapeutics* 271:1383–1390.
536 Felder CC, Joyce KE, Briley EM, Mansouri J, Mackie K, Blond O, Lai Y, Ma AL, Mitchell RL.
537 1995. Comparison of the pharmacology and signal transduction of the human cannabinoid
538 CB1 and CB2 receptors. *Molecular Pharmacology* 48:443–450.
539 Feng Y-J, Li Y-Y, Lin X-H, Li K, Cao M-H. 2016. Anti-inflammatory effect of cannabinoid
540 agonist WIN55, 212 on mouse experimental colitis is related to inhibition of p38MAPK.
541 *World Journal of Gastroenterology* 22:9515–9524. DOI: 10.3748/wjg.v22.i43.9515.

542 Freichel M, Berlin M, Schürger A, Mathar I, Bacmeister L, Medert R, Frede W, Marx A, Segin
543 S, Londoño JEC. 2017. TRP Channels in the Heart. In: Emir TLR ed. *Neurobiology of TRP*
544 *Channels*. Frontiers in Neuroscience. Boca Raton (FL): CRC Press/Taylor & Francis,.
545 Gheblawi M, Wang K, Viveiros A, Nguyen Q, Zhong J-C, Turner AJ, Raizada MK, Grant MB,
546 Oudit GY. 2020. Angiotensin-Converting Enzyme 2: SARS-CoV-2 Receptor and
547 Regulator of the Renin-Angiotensin System: Celebrating the 20th Anniversary of the
548 Discovery of ACE2. *Circulation Research* 126:1456–1474. DOI:
549 10.1161/CIRCRESAHA.120.317015.
550 Gomes IC, Karmirian K, Oliveira J, Pedrosa C, Rosman FC, Chimelli L, Rehen S. 2020. SARS-
551 CoV-2 Infection in the Central Nervous System of a 1-Year-Old Infant Submitted to
552 Complete Autopsy. DOI: 10.20944/preprints202009.0297.v1.
553 Guo J, Huang Z, Lin L, Lv J. 2020. Coronavirus Disease 2019 (COVID-19) and Cardiovascular
554 Disease: A Viewpoint on the Potential Influence of Angiotensin-Converting Enzyme
555 Inhibitors/Angiotensin Receptor Blockers on Onset and Severity of Severe Acute
556 Respiratory Syndrome Coronavirus 2 Infection. *Journal of the American Heart Association*
557 9:e016219. DOI: 10.1161/JAHA.120.016219.
558 Huentelman MJ, Grobe JL, Vazquez J, Stewart JM, Mecca AP, Katovich MJ, Ferrario CM,
559 Raizada MK. 2005. Protection from angiotensin II-induced cardiac hypertrophy and
560 fibrosis by systemic lentiviral delivery of ACE2 in rats. *Experimental Physiology* 90:783–
561 790. DOI: 10.1113/expphysiol.2005.031096.
562 Jeske NA, Patwardhan AM, Gamper N, Price TJ, Akopian AN, Hargreaves KM. 2006.
563 Cannabinoid WIN 55,212-2 regulates TRPV1 phosphorylation in sensory neurons. *The*
564 *Journal of Biological Chemistry* 281:32879–32890. DOI: 10.1074/jbc.M603220200.
565 Jiang S, Fu Y, Williams J, Wood J, Pandarinathan L, Avraham S, Makriyannis A, Avraham S,
566 Avraham HK. 2007. Expression and Function of Cannabinoid Receptors CB1 and CB2
567 and Their Cognate Cannabinoid Ligands in Murine Embryonic Stem Cells. *PLOS ONE*
568 2:e641. DOI: 10.1371/journal.pone.0000641.

569 Keck M, Flamant M, Mougenot N, Favier S, Atassi F, Barbier C, Nadaud S, Lompré A-M, Hulot
570 J-S, Pavoine C. 2019. Cardiac inflammatory CD11b/c cells exert a protective role in
571 hypertrophied cardiomyocyte by promoting TNFR 2 - and Orai3- dependent signaling.
572 *Scientific Reports* 9:6047. DOI: 10.1038/s41598-019-42452-y.
573 Kleinbongard P, Schulz R, Heusch G. 2011. TNFα in myocardial ischemia/reperfusion,
574 remodeling and heart failure. *Heart Failure Reviews* 16:49–69. DOI: 10.1007/s10741-010-
575 9180-8.
576 Koch M, Kreutz S, Böttger C, Grabiec U, Ghadban C, Korf H-W, Dehghani F. 2011. The
577 cannabinoid WIN 55,212-2-mediated protection of dentate gyrus granule cells is driven by
578 CB1 receptors and modulated by TRPA1 and Cav 2.2 channels. *Hippocampus* 21:554–
579 564. DOI: 10.1002/hipo.20772.
580 Kwon Y, Nukala SB, Srivastava S, Miyamoto H, Ismail NI, Jousma J, Rehman J, Ong S-B,
581 Lee WH, Ong S-G. 2020. Detection of viral RNA fragments in human iPSC
582 cardiomyocytes following treatment with extracellular vesicles from SARS-CoV-2 coding
583 sequence overexpressing lung epithelial cells. *Stem Cell Research & Therapy* 11:514.
584 DOI: 10.1186/s13287-020-02033-7.
585 Lei X, Dong X, Ma R, Wang W, Xiao X, Tian Z, Wang C, Wang Y, Li L, Ren L, Guo F, Zhao
586 Z, Zhou Z, Xiang Z, Wang J. 2020. Activation and evasion of type I interferon responses
587 by SARS-CoV-2. *Nature Communications* 11. DOI: 10.1038/s41467-020-17665-9.
588 Lindner D, Fitzek A, Bräuninger H, Aleshcheva G, Edler C, Meissner K, Scherschel K, Kirchhof
589 P, Escher F, Schultheiss H-P, Blankenberg S, Püschel K, Westermann D. 2020.
590 Association of Cardiac Infection With SARS-CoV-2 in Confirmed COVID-19 Autopsy
591 Cases. *JAMA Cardiology* 5:1281. DOI: 10.1001/jamacardio.2020.3551.
592 Mahé A, Birckel E, Krieger S, Merklen C, Bottlaender L. 2020. A distinctive skin rash
593 associated with coronavirus disease 2019? *Journal of the European Academy of*
594 *Dermatology and Venereology: JEADV* 34:e246–e247. DOI: 10.1111/jdv.16471.
595 Maisch B. 2020. SARS-CoV-2 as potential cause of cardiac inflammation and heart failure. Is
596 it the virus, hyperinflammation, or MODS? *Herz*:1–2. DOI: 10.1007/s00059-020-04925-z.

Marchalant Y, Rosi S, Wenk GL. 2007. Anti-inflammatory property of the cannabinoid agonist WIN-55212-2 in a rodent model of chronic brain inflammation. *Neuroscience* 144:1516–1522. DOI: 10.1016/j.neuroscience.2006.11.016.

Meckiff BJ, Ramírez-Suástegui C, Fajardo V, Chee SJ, Kusnadi A, Simon H, Eschweiler S, Grifoni A, Pelosi E, Weiskopf D, Sette A, Ay F, Seumois G, Ottensmeier CH, Vijayanand P. 2020. Imbalance of Regulatory and Cytotoxic SARS-CoV-2-Reactive CD4+ T Cells in COVID-19. *Cell* 183:1340-1353.e16. DOI: 10.1016/j.cell.2020.10.001.

Medina-Vera D, Rosell-Valle C, López-Gambero AJ, Navarro JA, Zambrana-Infantes EN, Rivera P, Santín LJ, Suarez J, Rodríguez de Fonseca F. 2020. Imbalance of Endocannabinoid/Lysophosphatidylinositol Receptors Marks the Severity of Alzheimer's Disease in a Preclinical Model: A Therapeutic Opportunity. *Biology* 9:377. DOI: 10.3390/biology9110377.

Mendizábal VE, Adler-Graschinsky E. 2007. Cannabinoids as therapeutic agents in cardiovascular disease: a tale of passions and illusions. *British Journal of Pharmacology* 151:427–440. DOI: 10.1038/sj.bjp.0707261.

Miklós Z, Wafa D, Nádasy GL, Tóth ZE, Besztercei B, Dörnyei G, Laska Z, Benyó Z, Ivanics T, Hunyady L, Szekeres M. 2021. Angiotensin II-Induced Cardiac Effects Are Modulated by Endocannabinoid-Mediated CB1 Receptor Activation. *Cells* 10:724. DOI: 10.3390/cells10040724.

Mukhopadhyay P, Rajesh M, Bátkai S, Patel V, Kashiwaya Y, Liaudet L, Evgenov OV, Mackie K, Haskó G, Pacher P. 2010. CB1 cannabinoid receptors promote oxidative stress and cell death in murine models of doxorubicin-induced cardiomyopathy and in human cardiomyocytes. *Cardiovascular Research* 85:773–784. DOI: 10.1093/cvr/cvp369.

Munro S, Thomas KL, Abu-Shaar M. 1993. Molecular characterization of a peripheral receptor for cannabinoids. *Nature* 365:61–65. DOI: 10.1038/365061a0.

Nguyen LC, Yang D, Nicolaescu V, Best TJ, Ohtsuki T, Chen S-N, Friesen JB, Drayman N, Mohamed A, Dann C, Silva D, Gula H, Jones KA, Millis JM, Dickinson BC, Tay S, Oakes SA, Pauli GF, Meltzer DO, Randall G, Rosner MR. 2021. Cannabidiol Inhibits SARS-CoV-

2 Replication and Promotes the Host Innate Immune Response. *bioRxiv*:2021.03.10.432967. DOI: 10.1101/2021.03.10.432967.

Pacher P, Steffens S, Haskó G, Schindler TH, Kunos G. 2018. Cardiovascular effects of marijuana and synthetic cannabinoids: the good, the bad, and the ugly. *Nature Reviews Cardiology* 15:151–166. DOI: 10.1038/nrcardio.2017.130.

Perez-Bermejo JA, Kang S, Rockwood SJ, Simoneau CR, Joy DA, Silva AC, Ramadoss GN, Flanigan WR, Fozouni P, Li H, Chen P-Y, Nakamura K, Whitman JD, Hanson PJ, McManus BM, Ott M, Conklin BR, McDevitt TC. 2021. SARS-CoV-2 infection of human iPSC–derived cardiac cells reflects cytopathic features in hearts of patients with COVID-19. *Science Translational Medicine* 13. DOI: 10.1126/scitranslmed.abf7872.

Puelles VG, Lütgehetmann M, Lindenmeyer MT, Sperhake JP, Wong MN, Allweiss L, Chilla S, Heinemann A, Wanner N, Liu S, Braun F, Lu S, Pfefferle S, Schröder AS, Edler C, Gross O, Glatzel M, Wichmann D, Wiech T, Kluge S, Pueschel K, Aepfelbacher M, Huber TB. 2020. Multiorgan and Renal Tropism of SARS-CoV-2. *New England Journal of Medicine* 383:590–592. DOI: 10.1056/NEJMc2011400.

Rahmatollahi M, Baram SM, Rahimian R, Saeedi Saravi SS, Dehpour AR. 2016. Peroxisome Proliferator-Activated Receptor-α Inhibition Protects Against Doxorubicin-Induced Cardiotoxicity in Mice. *Cardiovascular Toxicology* 16:244–250. DOI: 10.1007/s12012-015-9332-0.

Ramirez SH, Reichenbach NL, Fan S, Rom S, Merkel SF, Wang X, Ho W-Z, Persidsky Y. 2013. Attenuation of HIV-1 replication in macrophages by cannabinoid receptor 2 agonists. *Journal of Leukocyte Biology* 93:801–810. DOI: 10.1189/jlb.1012523.

Reiss CS. 2010. Cannabinoids and Viral Infections. *Pharmaceuticals* 3:1873–1886. DOI: 10.3390/ph3061873.

Rossi F, Tortora C, Argenziano M, Di Paola A, Punzo F. 2020. Cannabinoid Receptor Type 2: A Possible Target in SARS-CoV-2 (CoV-19) Infection? *International Journal of Molecular Sciences* 21. DOI: 10.3390/ijms21113809.

652 Sachdev S, Vemuri K, Banister SD, Longworth M, Kassiou M, Santiago M, Makriyannis A,
653 Connor M. 2019. In vitro determination of the efficacy of illicit synthetic cannabinoids at
654 CB1 receptors. *British Journal of Pharmacology* 176:4653–4665. DOI:
655 10.1111/bph.14829.
656 Sainz-Cort A, Heeroma JH. 2020. The interaction between the endocannabinoid system and
657 the renin angiotensin system and its potential implication for COVID-19 infection. *Journal*
658 *of Cannabis Research* 2:23. DOI: 10.1186/s42238-020-00030-4.
659 Salerno JA, Torquato T, Temerozo JR, Goto-Silva L, Mendes M, Sacramento CQ, Fintelman-
660 Rodrigues N, Vitoria G, Souza L, Ornelas I, Veríssimo C, Karmirian K, Pedrosa C, Dias S
661 da SG, Soares VC, Aragão LGH, Puig-Pijuan T, Salazar VW, Dariolli R, Biagi D, Furtado
662 DR, Borges HL, Bozza P, Guimarães MZ, Souza TML, Rehen SK. 2021. Inhibition of
663 SARS-CoV-2 infection in human cardiomyocytes by targeting the Sigma-1 receptor
664 disrupts cytoskeleton architecture and contractility. *bioRxiv*:2021.02.20.432092. DOI:
665 10.1101/2021.02.20.432092.
666 Sharma A, Garcia G, Wang Y, Plummer JT, Morizono K, Arumugaswami V, Svendsen CN.
667 2020. Human iPSC-Derived Cardiomyocytes Are Susceptible to SARS-CoV-2 Infection.
668 *Cell Reports Medicine* 1:100052. DOI: 10.1016/j.xcrm.2020.100052.
669 Shmist YA, Goncharov I, Eichler M, Shneyvays V, Isaac A, Vogel Z, Shainberg A. 2006. Delta-
670 9-tetrahydrocannabinol protects cardiac cells from hypoxia via CB2 receptor activation
671 and nitric oxide production. *Molecular and Cellular Biochemistry* 283:75–83. DOI:
672 10.1007/s11010-006-2346-y.
673 Smeets PJH, Teunissen BEJ, Planavila A, de Vogel-van den Bosch H, Willemsen PHM, van
674 der Vusse GJ, van Bilsen M. 2008. Inflammatory Pathways Are Activated during
675 Cardiomyocyte Hypertrophy and Attenuated by Peroxisome Proliferator-activated
676 Receptors PPARα and PPARδ. *The Journal of Biological Chemistry* 283:29109–29118.
677 DOI: 10.1074/jbc.M802143200.
678 Smith SR, Terminelli C, Denhardt G. 2000. Effects of cannabinoid receptor agonist and
679 antagonist ligands on production of inflammatory cytokines and anti-inflammatory

680 interleukin-10 in endotoxemic mice. *The Journal of Pharmacology and Experimental*
681 *Therapeutics* 293:136–150.
682 Soethoudt M, Grether U, Fingerle J, Grim TW, Fezza F, de Petrocellis L, Ullmer C,
683 Rothenhäusler B, Perret C, van Gils N, Finlay D, MacDonald C, Chicca A, Gens MD,
684 Stuart J, de Vries H, Mastrangelo N, Xia L, Alachouzos G, Baggelaar MP, Martella A,
685 Mock ED, Deng H, Heitman LH, Connor M, Di Marzo V, Gertsch J, Lichtman AH,
686 Maccarrone M, Pacher P, Glass M, van der Stelt M. 2017. Cannabinoid CB 2 receptor
687 ligand profiling reveals biased signalling and off-target activity. *Nature Communications*
688 8:13958. DOI: 10.1038/ncomms13958.
689 Tahamtan A, Tavakoli-Yaraki M, Rygiel TP, Mokhtari-Azad T, Salimi V. 2016. Effects of
690 cannabinoids and their receptors on viral infections. *Journal of Medical Virology* 88:1–12.
691 DOI: 10.1002/jmv.24292.
692 Thum T. 2020. SARS-CoV-2 receptor ACE2 expression in the human heart: cause of a post-
693 pandemic wave of heart failure? *European Heart Journal* 41:1807–1809. DOI:
694 10.1093/eurheartj/ehaa410.
695 Unudurthi SD, Luthra P, Bose RJC, McCarthy JR, Kontaridis MI. 2020. Cardiac inflammation
696 in COVID-19: Lessons from heart failure. *Life Sciences* 260:118482. DOI:
697 10.1016/j.lfs.2020.118482.
698 Varga Z, Flammer AJ, Steiger P, Haberecker M, Andermatt R, Zinkernagel AS, Mehra MR,
699 Schuepbach RA, Ruschitzka F, Moch H. 2020. Endothelial cell infection and endotheliitis
700 in COVID-19. *The Lancet* 395:1417–1418. DOI: 10.1016/S0140-6736(20)30937-5.
701 Wang B, Kovalchuk A, Li D, Rodriguez-Juarez R, Ilnytskyy Y, Kovalchuk I, Kovalchuk O. 2020.
702 In search of preventive strategies: novel high-CBD Cannabis sativa extracts modulate
703 ACE2 expression in COVID-19 gateway tissues. *Aging* 12:22425–22444. DOI:
704 10.18632/aging.202225.
705 Wang J-H, Zhao L, Pan X, Chen N-N, Chen J, Gong Q-L, Su F, Yan J, Zhang Y, Zhang S-H.
706 2016. Hypoxia-stimulated cardiac fibroblast production of IL-6 promotes myocardial

fibrosis via the TGF- β 1 signaling pathway. *Laboratory Investigation* 96:839–852. DOI: 10.1038/labinvest.2016.65.

Wenzel DG. 1967. Drug-induced cardiomyopathies. *Journal of Pharmaceutical Sciences* 56:1209–1224. DOI: 10.1002/jps.2600561002.

Wong C-K, Luk HK-H, Lai W-H, Lau Y-M, Zhang RR, Wong AC-P, Lo GC-S, Chan K-H, Hung IF-N, Tse H-F, Woo PC-Y, Lau SK-P, Siu C-W. 2020. Human-Induced Pluripotent Stem Cell-Derived Cardiomyocytes Platform to Study SARS-CoV-2 Related Myocardial Injury. *Circulation Journal: Official Journal of the Japanese Circulation Society* 84:2027–2031. DOI: 10.1253/circj.CJ-20-0881.

Yamauchi-Takihara K, Ihara Y, Ogata A, Yoshizaki K, Azuma J, Kishimoto T. 1995. Hypoxic stress induces cardiac myocyte-derived interleukin-6. *Circulation* 91:1520–1524. DOI: 10.1161/01.cir.91.5.1520.

Yan R, Zhang Y, Li Y, Xia L, Guo Y, Zhou Q. 2020. Structural basis for the recognition of SARS-CoV-2 by full-length human ACE2. *Science* 367:1444–1448. DOI: 10.1126/science.abb2762.

Zheng Y-Y, Ma Y-T, Zhang J-Y, Xie X. 2020. COVID-19 and the cardiovascular system. *Nature Reviews Cardiology* 17:259–260. DOI: 10.1038/s41569-020-0360-5.

Zhong J, Basu R, Guo D, Chow FL, Byrns S, Schuster M, Loibner H, Wang X, Penninger JM, Kassiri Z, Oudit GY. 2010. Angiotensin-converting enzyme 2 suppresses pathological hypertrophy, myocardial fibrosis, and cardiac dysfunction. *Circulation* 122:717–728, 18 p following 728. DOI: 10.1161/CIRCULATIONAHA.110.955369.

Zhou B, She J, Wang Y, Ma X. 2020. The clinical characteristics of myocardial injury in severe and very severe patients with 2019 novel coronavirus disease. *The Journal of Infection* 81:147–178. DOI: 10.1016/j.jinf.2020.03.021.

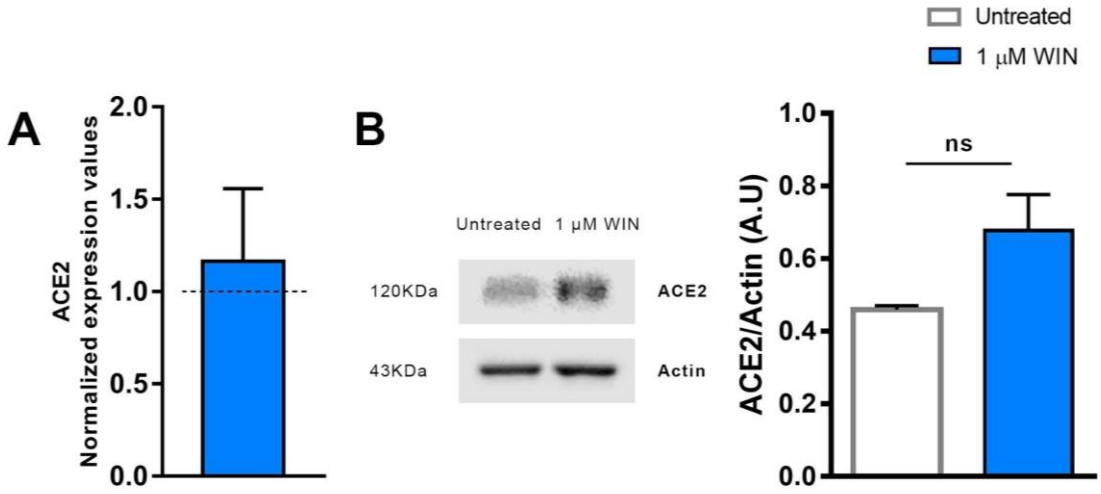

Figure 1. WIN does not modulate ACE2 in hiPSC-CMs. (A) Relative mRNA expression levels of ACE2 in WIN-treated hiPSC-CMs expressed as fold change relative to untreated condition. (B) Quantification of western blots by densitometry normalized by actin expression. ACE2 mRNA and protein levels were comparable between WIN-treated and untreated hiPSC-CMs. Error bars represent standard errors of the means (SEMs) from three (A) and four (B) independent experiments (3 or 4 cellular differentiation) from one cell line.

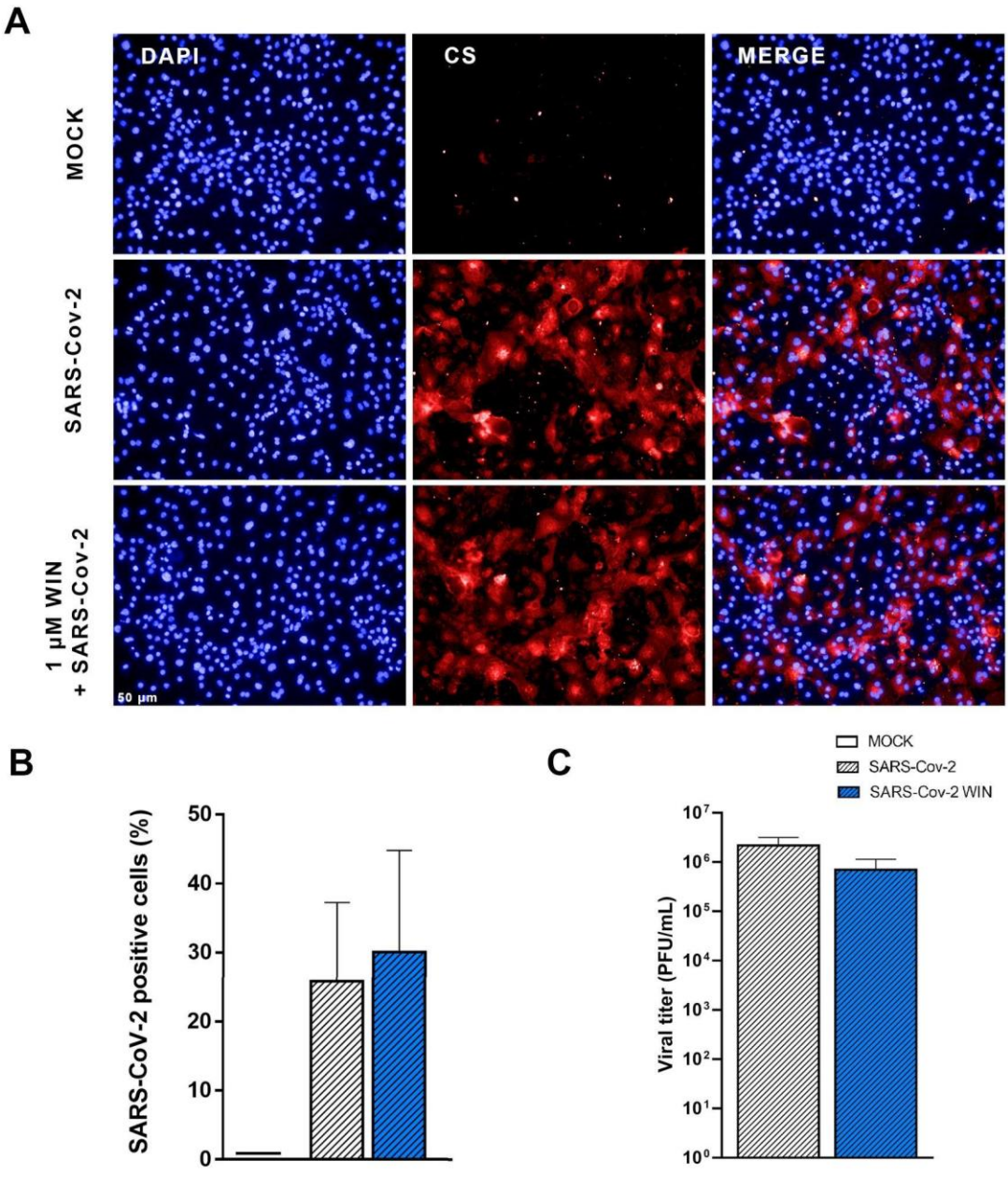

746

747 **Figure 2.** WIN does not reduce SARS-CoV-2 infection and replication in hiPSC-CMs. (A)
748 Representative micrographs of MOCK and SARS-CoV-2-infected hiPSC-CM pre-treated or
749 not with 1 µM WIN for 24 hours. hiPSC-CM were immunostained with SARS-CoV-2
750 convalescent serum (CS) (red) and counterstained with DAPI (blue) at 48h post-infection.
751 Scale bar: 50 µm. (B) Percentage of CS positive cells. CS immunoreactivity was comparable
752 between treated and untreated hiPSC-CM. (C) Viral titer quantification by plaque forming units
753 assay using the supernatants of the SARS-CoV-2 infected hiPSC-CMs. Viral titer was
754 comparable between treated and untreated hiPSC-CM. Error bars represent standard errors
755 of the means (SEM) from three independent experiments (3 cellular differentiations and 3
756 independent infections) from one iPSC line.

757

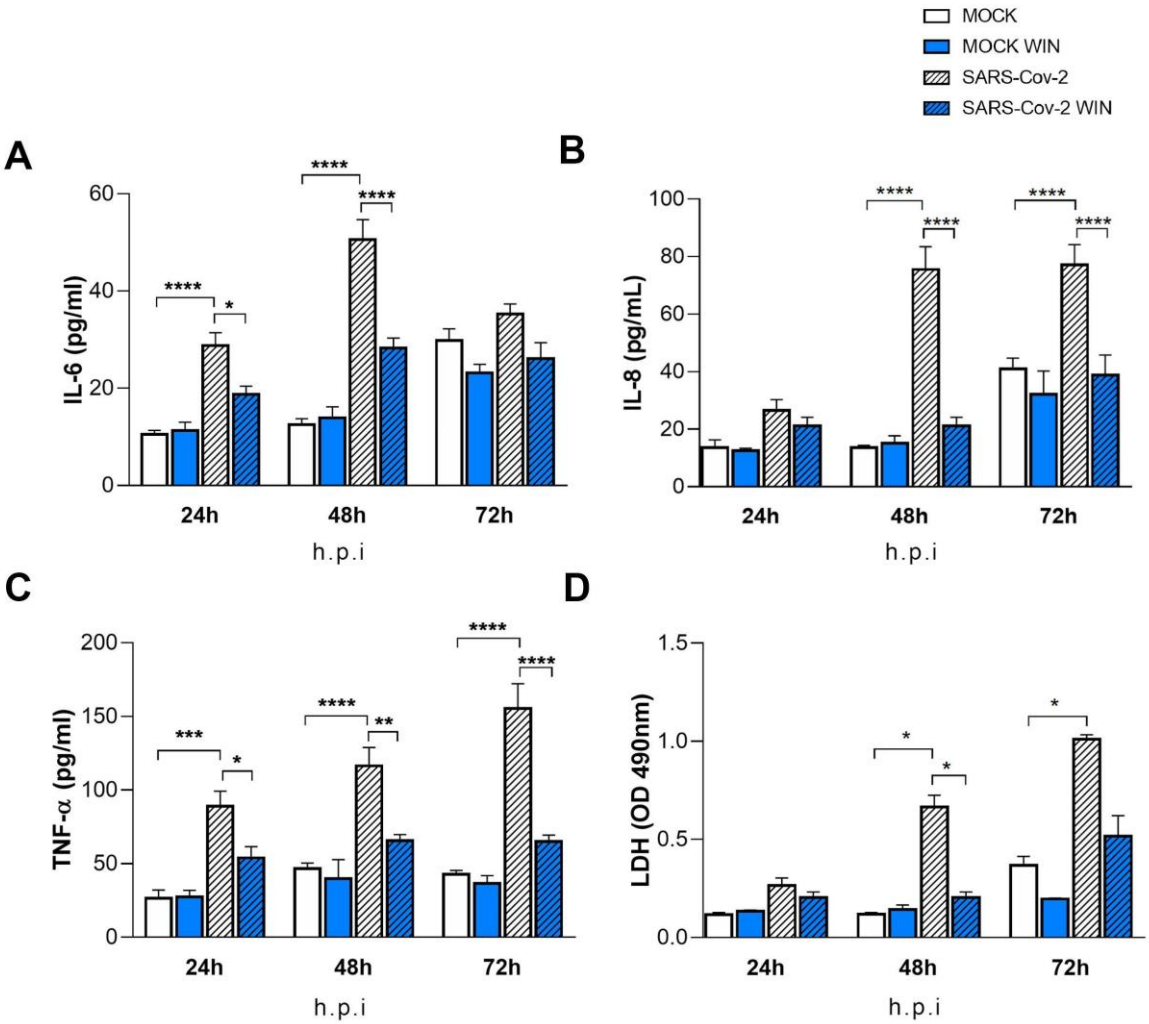

Figure 3. WIN reduces inflammatory markers and viral toxicity in hiPSC-CMs. Levels of IL-6 (A), IL-8 (B), TNF-α (C), and (D) release of lactate dehydrogenase (LDH) from MOCK and SARS-CoV-2-infected hiPSC-CM, treated or not with 1 μM WIN for 24 hours, were analyzed at 24-, 48- and 72-hours post-infection (h.p.i.). Cytokine levels were higher in SARS-CoV-2 compared with control (MOCK), and lower in SARS-CoV-2 WIN when compared with SARS-CoV-2. LDH release-absorbance levels relative to MOCK was higher in SARS-CoV-2 compared with SARS-CoV-2 WIN. Data represent means and standard errors of the means (SEM) from three independent experiments from one cell line. *$p < 0.05$, **$p < 0.01$, ***$p < 0.001$, **** $p < 0.0001$.

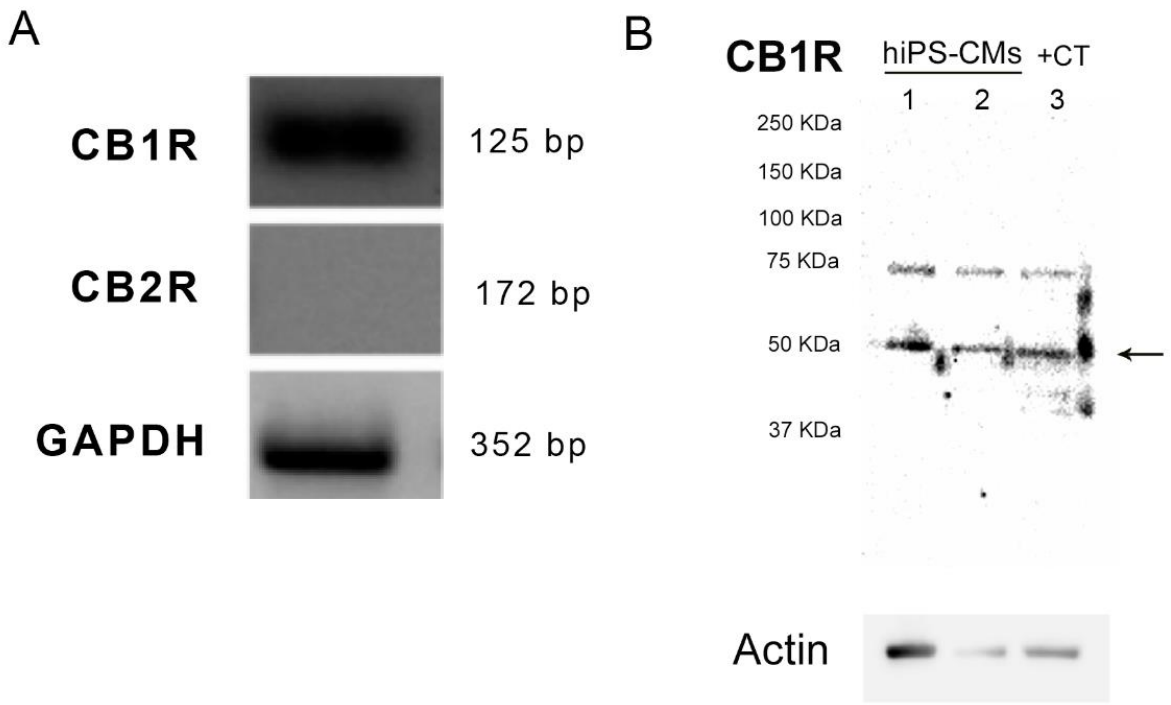

771

772 **Fig S1**. CB1 and CB2 receptors expression. (A) The figure shows agarose gel of end-point
773 PCR products for cDNA from hiPSC-CMs. One single specific band was detected for CB1
774 receptor (125bp), while no such band was detected for CB2 receptor (172 bp). GAPDH (352
775 bp) was used as an endogenous control to confirm efficiency of the amplification reaction and
776 quality of cDNA template. Data from two independent experiments. (B) Western blot detection
777 of CB1 receptor protein levels in hiPSC-CMs. The arrows indicate the specific bands,
778 corresponding to the molecular weight predicted to CB1 receptor. hiPSC-CMs samples were
779 taken from different passages and the positive control (CT) was from tissue homogenates of
780 adult Black C57/BL6 mouse hippocampus.

781

782

783

784

785

786

787

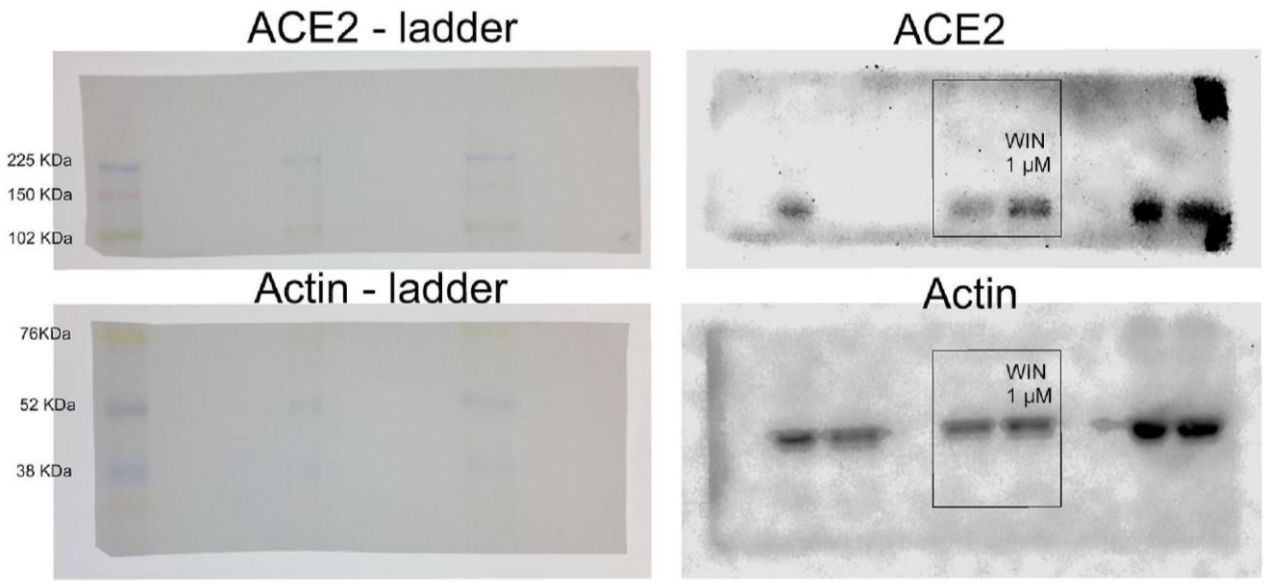

Fig S2. Full-length gels for western blot detection of ACE2 in untreated and WIN treated hiPSC-CMs. After transference the membrane was cut, the upper half used for ACE2 detection, and the bottom half used for actin detection. Images of the membranes used for detection with the ladder (Amersham ECL Rainbow Marker - Full range) are shown on the left. Full-length gels for ACE2 and actin with contrast adjusted to allow visualization of the membrane are shown on the right. Although the whole gel is shown here the lanes used for representative image in Fig 1 are highlighted in a box. Other lanes have samples that are not related to the experiment in this manuscript.

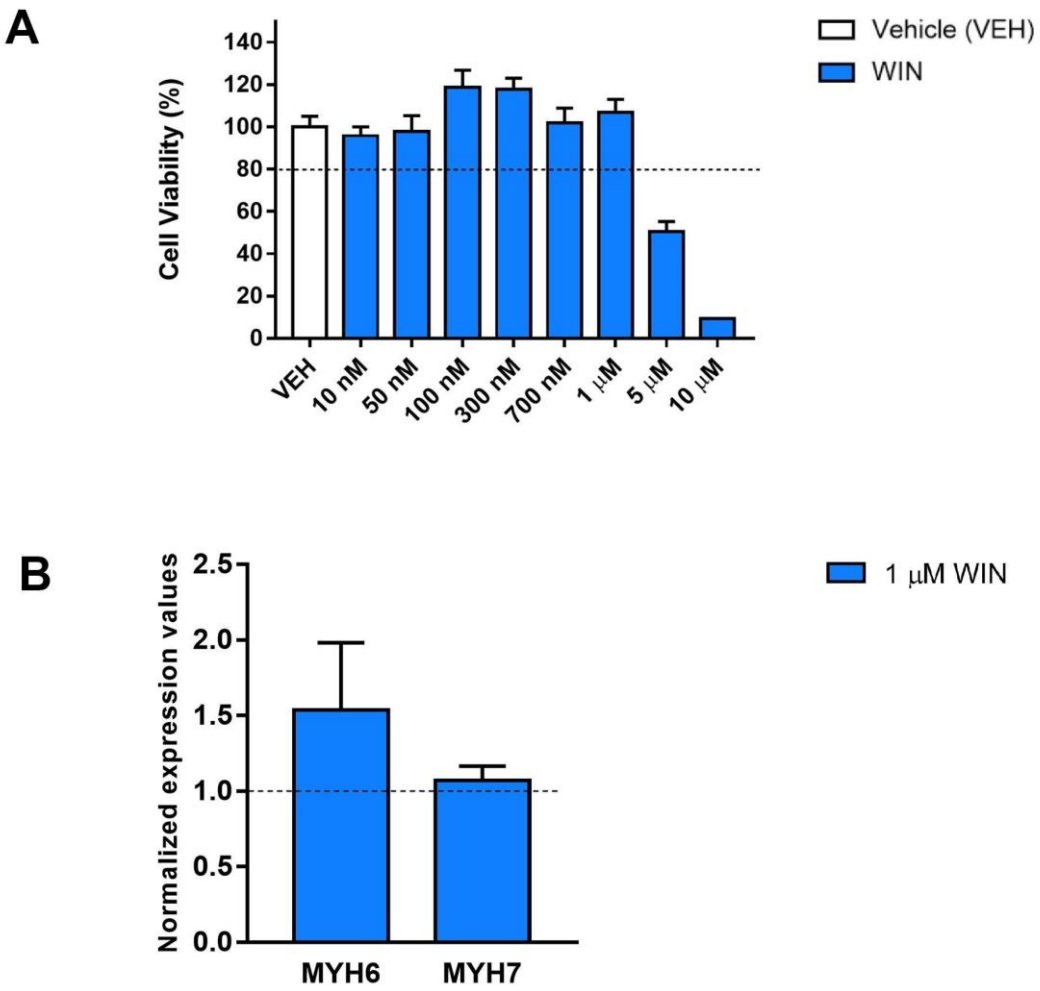

803 **Fig S3**. Cell viability assay and quantitative real-time PCR for genes correlated to
804 hypertrophy. (A) Neutral red uptake assay from hiPSC-CMs treated with increasing
805 concentrations of WIN for 72 hours. The highest non-cytotoxic concentration was 1
806 μM. (B). qPCR for MYH6 and MYH7 genes from hiPSC-CMs treated with 1μM WIN
807 for 24 hours. The MYH6 and MYH7 levels showed no significant differences between
808 WIN-treated and untreated cells.

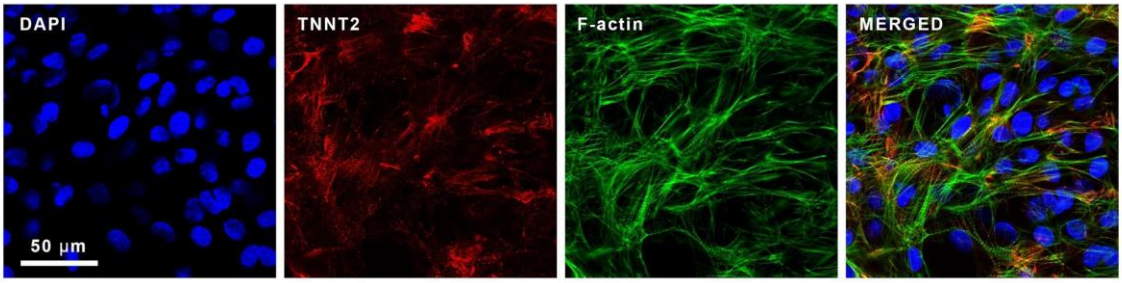

Fig S4. Micrographs of hiPSC-CMs immunostained for cTnT. hiPSC-CMs were immunostained for TNNT2 (red), filamentous actin (F-actin) (green) by phalloidin staining and counterstained with DAPI (blue); 63x magnification; Scale bar: 50 µm.